Malaysian Journal of Analytical Sciences (MJAS)



Published by Malaysian Analytical Sciences Society

SPECTROSCOPIC, CRYSTAL STRUCTURE, HIRSHFELD SURFACE AND DFT STUDIES OF 2-AMINO-4-CHLOROBENZONITRILE

(Kajian Spektroskopi, Struktur Hablur, Permukaan Hirsfeld dan DFT bagi 2-Amino-4-Klorobenzonitril)

Onur Erman Dogan¹, Erbil Agar¹, Necmi Dege², Erna Normaya⁴, Siti Syaida Sirat^{3,5}, and Nur Nadia Dzulkifli^{3*}

¹Department of Chemistry, Faculty of Arts and Sciences, Ondokuz Mayıs University, Samsun, Turkey

²Department of Physics, Faculty of Arts and Sciences, Ondokuz Mayıs University, Samsun, Turkey

³School of Chemistry and Environment, Faculty of Applied Sciences, Universiti Teknologi MARA Cawangan Negeri Sembilan,
Kampus Kuala Pilah, Pekan Parit Tinggi, 72000 Kuala Pilah, Negeri Sembilan, Malaysia

⁴Experimental and Theoretical Research Laboratory, Department of Chemistry, Kulliyyah of Science, International Islamic
University Malaysia, Jalan Sultan Haji Ahmad Shah, Bandar Indera Mahkota, 25200, Kuantan, Pahang, Malaysia

⁵Atta-ur-Rahman Institute for Natural Product Discovery (AuRIns), Universiti Teknologi MARA, Kampus Puncak Alam, 42300

Bandar Puncak Alam, Selangor, Malaysia

*Corresponding author: nurnadia@uitm.edu.my

Received: 2 July 2023; Accepted: 4 November 2023; Published: 28 February 2024

Abstract

This research concentrates on a summary of the global reactivity parameters on the single crystal structure of 2-amino-4chlorobenzonitrile, which can be utilised in a wide range of applications. The commercial 2-amino-4-chlorobenzonitrile in light yellow (Sigma-Aldrich) [ACBN] was recrystallized from ethanol. The compound crystallizes in the triclinic, P-1 space group with unit cell parameters a = 3.8924 (9) Å, b = 6.7886 (15) Å, c = 13.838 (3) Å, $\alpha = 77.559$ (16)°, $\beta = 8.898$ (17)° and $\gamma = 83.021$ (17)°. The presence of intermolecular interactions was further analyzed via the Hirshfeld Surface analysis. The electronic properties of the compound were investigated via the Density Functional Theory (DFT) using the CIF file of the single crystal. Full geometry optimization was carried out using the DFT at B3LYP with 6-311++G (d, p) basis set level. The structure of the recrystallized ACBN was confirmed via single crystal X-ray Crystallography, FTIR, and UV-Vis. The IR spectrum showed three main stretching bands namely nitrile, C≡N (2211 cm⁻¹), C-Cl (782 cm⁻¹), and 1° NH (3452 and 3363 cm⁻¹). The UV-Vis analysis showed two main absorption peaks namely $\pi \to \pi *$ and $n \to \pi *$ which occurred in an aromatic ring and nitrile, C=N. The compound crystallized in the triclinic system with the space group Pī. Nitrile (C≡N) and C-N have bond lengths of 1.146(4) and 1.369(4) Å, which are less than the theoretical values of 1.160 and 1.470 Å due to the conjugation of the aromatic ring. The intrinsic molecular characteristics analysis showed that the compound has the capability to donate electrons although it is categorized as a hard compound. The exploration of intrinsic molecular features revealed that, despite the fact that ACBN is stable and less reactive, it still has the ability to transfer and accept electrons. Furthermore, the Mulliken analysis revealed that the compound has the capability to function as a nucleophilic agent due to the nitrogen atoms (highly negative charges). As recommendation, the DFT study revealed that the compound can be investigated more thoroughly in terms of reaction kinetics and mechanisms such as corrosion inhibition and biological activities.

Keywords: benzonitrile, density functional theory, mulliken, molecular electrostatic potential, Hirshfeld surface

Abstrak

Kajian ini menumpukan kepada ringkasan parameter kereaktifan global bagi struktur hablur tunggal 2-amino-4-klorobenzonitril, yang boleh diaplikasikan dalam pelbagai kegunaan. Komersial 2-amino-4-klorobenzonitril yang berwarna kuning cair (Sigma-Aldrich) [ACBN] telah dilakukan penghabluran semula daripada etanol. Sebatian tersebut menghablur dalam triklinik, kumpulan ruang P-1 dengan parameter sel unit a = 3.8924 (9) Å, b = 6.7886 (15) Å, c = 13.838 (3) Å, $\alpha = 77.559$ (16)°, $\beta = 8.898$ (17)° and $\gamma = 83.021 (17)^{\circ}$. Kewujudan interaksi antara molekul dianalisis selanjutnya dengan Permukaan Hirshfeld. Sifat elektronik sebatian telah dikaji dengan Teori Fungsian Ketumpatan (DFT) menggunakan fail CIF hablur tunggal. Pengoptimuman geometri penuh sebatian telah dilakukan menggunakan B3LYP dengan tahap asas 6-311++G (d, p). Struktur hablur ACBN telah disahkan melalui Kristalografi sinar-X hablur tunggal, FTIR, dan UV-Vis. Spektrum IR menunjukkan tiga jalur regangan yang utama iaitu nitril, C≡N (2211 cm⁻¹), C-Cl (782 cm⁻¹), dan 1° NH (3452 dan 3363 cm⁻¹). Analisis UV-Vis menunjukkan dua puncak serapan utama iaitu $\pi \to \pi *$ dan $n \to \pi *$ yang wujud dalam gegelang aromatik dan nitril, $C \equiv N$. Sebatian itu terhablur dalam sistem triklinik dengan kumpulan ruang Pī. Nitril (C≡N) dan C-N mempunyai panjang ikatan iaitu 1.146(4) dan 1.369(4) Å di mana kurang daripada nilai teori iaitu 1.160 dan 1.470 Å disebabkan oleh konjugasi dalam gegelang aromatik. Analisis ciri molekul intrinsik menunjukkan bahawa sebatian ACBN mempunyai keupayaan untuk menderma elektron walaupun dikategorikan sebagai sebatian keras. Penerokaan ciri molekul intrinsik mendedahkan bahawa, walaupun hakikatnya ACBN adalah stabil dan kurang reaktif tapi masih mempunyai keupayaan menderma dan menerima elektron. Tambahan pula, analisis Mulliken mendedahkan bahawa sebatian tersebut mempunyai keupayaan untuk berfungsi sebagai agen nukleofilik disebabkan oleh atom nitrogen mempunyai cas negatif yang tinggi. Sebagai cadangan, analisis DFT mendedahkan bahawa sebatian ACBN boleh dikaji lebih teliti dari segi kinetik tindak balas kimia dan mekanisma seperti perencatan kakisan dan aktiviti biologi.

Kata kunci: benzonitril, teori fungsian ketumpatan, Mulliken, potensi elektrostatik molekul, permukaan Hirshfeld

Introduction

Benzonitrile (BN) is produced primarily by heating benzoic acid and theocyanate at 191°C. The liquid benzonitrile smells of almond and is clear and colorless. Due to its properties as an aprotic polar solvent, BN has been widely employed as a solvent in chemistry. In headspace and aqueous extract aromas, it is a powerful odorant. Derivatives of benzonitrile are used in the food preservation business as well as the dye industry to create aniline blue [1]. Besides that, in medicine, the primary byproducts of benzonitrile-benzoic acid are used as urinary antiseptics in salt form and bronchial tube disinfectants in vapor form. Nitrile derivatives have a wide range of industrial applications; for instance, phthalonitrile has been utilized as a precursor to phtalocyanide, a crucial component of dyes [2]. Lacquers, polymers, anhydrous metallic salts as well as medicinal, agrochemical, and other organic chemical intermediates are all generated from benzoinitrile (BN) and its derivatives [3]. Benzonitrile, which features an electron-donor CN substituent, is referred to as being bifunctional since it has the capability to interact with both the CN lone pair and the π -conjugated ring surfaces [4]. The cyano (C≡N) group is a versatile ligand that can serve as both an acceptor and a donor [5]. It is known that the C≡N stretching frequency of the nitrile group

changes from low to high depending on whether or not it interacts with a solvent that donates hydrogen bonds [6]. For the re-crystallized compound, Density Functional Theory (DFT) calculations utilizing the B3LYP level of theory and the LANL2DZ basis set were reported, including geometry optimization, vibrational frequency analysis, and electronic structures. This work concentrates on the DFT analysis, with data generated using single crystal data of 2-amino-4chlorobenzonitrile (CIF format). Although a previous study on DFT analysis by Sudha et al. (2011) was discussed, the researchers employed the proposed structure rather than single crystal data. It is clear that the DFT and Hirshfeld Surface analysis data generated using the CIF file is very different from the previous study. Besides that, the spectroscopic study of ACBN is also discussed in this work. The goal of studying the intrinsic molecular features of ACBN by DFT is to determine its potential to be used in corrosion inhibition, biological activity, energy storage, energy conversion, and other applications.

Materials and Methods

The commercial 2-amino-4-chlorobenzonitrile (Sigma-Aldrich) was recrystallized from ethanol.

Physical measurements

Using a Shimadzu FTIR-8900 spectrophotometer with KBr pellets, the IR spectrum of the compound was recorded in the range 4000-400 cm $^{-1}$. The ultraviolet absorption spectra of the compound were analyzed in the range 200-400 nm using a Unicam UV-Vis spectrophotometer device with a 10-mm quartz cell. The UV model was taken from a 2×10^{-5} M solution of the compound, dissolved in ethanol at 20° C.

Crystal structure determination

A yellow crystal with dimensions of 0.044 \times 0.285 \times 0.672 mm was mounted on the goniometer of a STOE IPDS II diffractometer. At room temperature (296 K), measurements were performed using graphite monochromate MoK α radiation ($\lambda = 0.71073$ Å). Reflections were gathered in the rotation mode and cell parameters were determined using the X-AREA software [7]. Absorption correction was achieved by the integration method via X-RED32 software [7]. SHELXS 97 [8] was used in the solvation of the structure by direct methods. All atoms except for hydrogens were refined anisotropically by the fullmatrix least squares procedure based on F2 using SHELXL-97 [8]. All H atoms were positioned geometrically and treated using a riding model, fixing the bond lengths at 0.86, 0.93, and 0.96 Å for NH, CH and CH₃, respectively. The program ORTEP-3 for windows [9] and MERCURY [10] was used in the preparation of the figures. The crystal data collection and refinement parameters are given in Table 2.

Hirshfeld surface analysis

The Hirshfeld surface analyses were done using the CrystalExplorer17.5 program [11]. The normalized contact distances (dnorm) were mapped into the Hirshfeld surface, which allowed the visualization of intermolecular interactions. The red color represents the closest contact because it indicates the sum of di (the distance from the surface to the nearest nucleus internal to the surface) and de (the distance from the surface to the nearest nucleus external to the surface) whereby de

is shorter than the sum of the relevant van der Waals radii. The blue and white color signify the negligible and weak intermolecular interactions, respectively. The two-dimensional fingerprint plots were used to quantify the various intermolecular interactions in the title compound.

Density functional theory

All computations were performed using the Gaussian09 software package. Full geometry optimization was carried out using the Density Function Theory at B3LYP with 6-311++G (d, p) basis set level. The Mullikan charge distributions of the investigated compound was also computed at the same level of method. The GaussView 5.0 program was used to construct the optimized molecular geometry, HOMO and LUMO electron distributions, and the HOMO-LUMO energy gap. The TD-DFT calculation was performed on the ethanol solvent using the IEPCM method.

Results and Discussion

Fourier transform infrared

Nitrile (C≡N) is allotted as a single, typically intense stretching band at 2211 cm⁻¹ (for cyano compounds). The C-Cl stretching vibration in the ACBN at 782 cm⁻¹ confirms that the halogen group in the para position is highlighted to the aromatic CN group [12]. Geethapriya et al. claimed that the CH in plane bending vibration is typically evident at 1300-1000 cm⁻¹ and the CH outplane is captured at 1000-750 cm⁻¹ [13]. The CH in plane and out-plane for the ACBN is displayed in Figure 1. The ACBN's FTIR spectroscopic results show that it has distinctive peaks at 3452 and 3363 cm⁻¹, which refer to the primary NH functional group [14]. Due to the presence of benzene ring C=C stretching vibrational bands, there is significant stretching frequency at 1433 and 1485 cm⁻¹. The stretching bands at 3100-3000 cm⁻¹ range is where pure C-H stretching vibrations of aromatic compounds predominate. However, the stretching frequency of the ACBN is slightly different from the report, caused by the presence of withdrawing group Cl at para position.

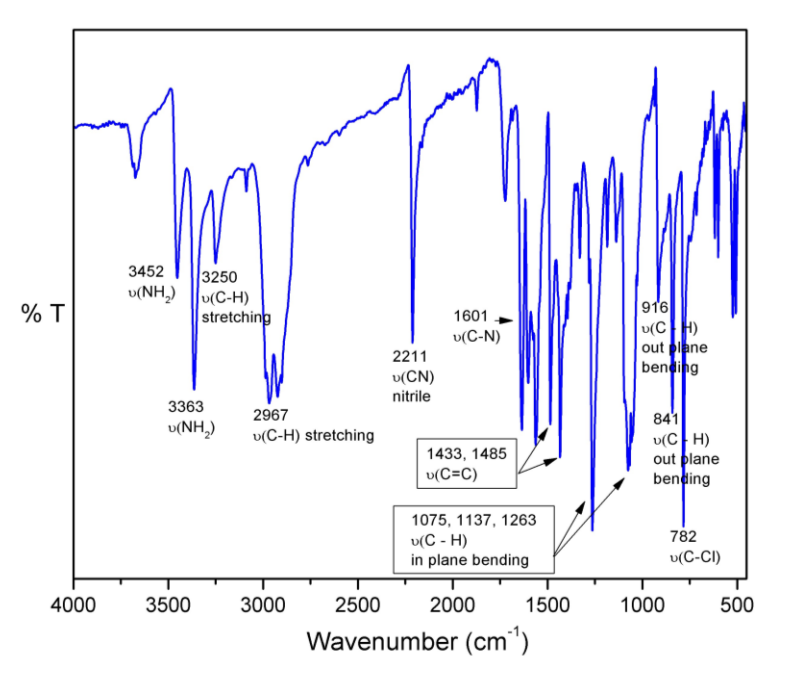


Figure 1. FTIR spectrum of ACBN

Ultraviolet-Visible

The ACBN absorption peak values are depicted in Figure 2. It is commonly perceived that the absorption peak approximately at 328 nm involve transition of $n\rightarrow\pi^*$ in the C \equiv N group. In contrast, the aromatic ring of $\pi\rightarrow\pi^*$ and $n\rightarrow\pi^*$ transitions may be accountable for the absorption peaks in the 210–400 nm range [15]. Figure 6 depicts the B3LYP frontier orbitals of ACBN, demonstrating that the HOMO and LUMO electrons were primarily localized across the whole ACBN where

the excitation process occurred. Besides that, based on the experimental and theoretical spectra, there are a slightly different number of absorption peaks. Changes in the geometry of the ACBN in the polar solvent (ethanol) would be associated with the creation of hydrogen bonds between ACBN-Ethanol. Hence, this will influence the electron localization in the HOMO-LUMO regions, causing the early absorption peak (TD-DFT) to be split into two peaks, as shown in Figure 2(a).

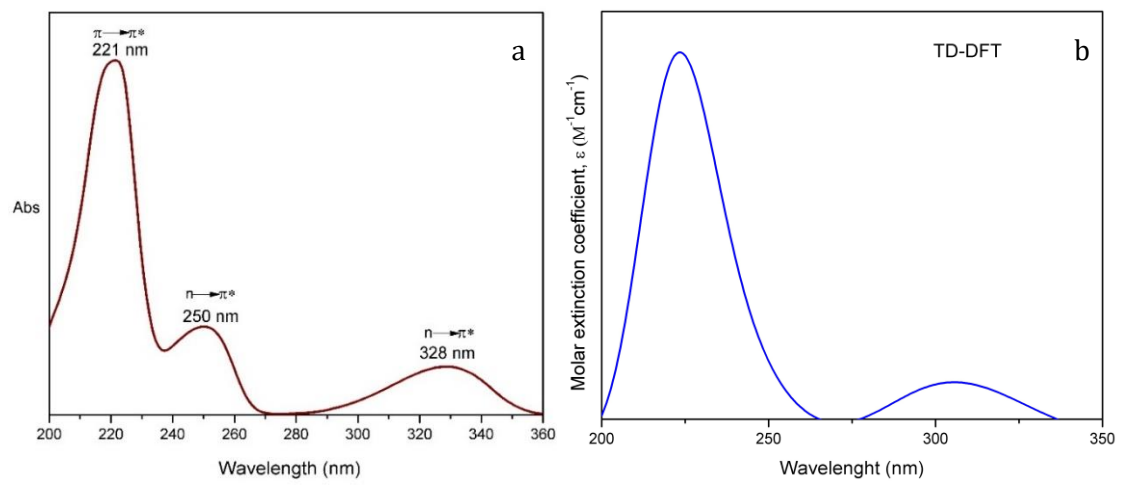


Figure 2. UV-Vis spectrum of ACBN; experimental (a) and theoretical (b)

Single crystal X-ray diffraction

This compound was obtained from the re-crystallization in ethanol. Figure 3 depicts the compound's crystal structure along with an atom-labelling system. The compound crystallized in the triclinic system with the space group Pī. Table 1 summarizes the key crystallographic information, in addition to the bond lengths and angles. Nitrile $(C \equiv N)$ and C-N have bond lengths of 1.146(4) and 1.369(4) Å, which are less than

the theoretical values of 1.160 and 1.470 Å due to the conjugation of the aromatic ring. Furthermore, the presence of the electron-withdrawing group, Cl, in the aromatic ring also led to the reduction of bond lengths. In the crystal structure of BN, the compounds were linked by intermolecular hydrogen bonds, N1---H1A---N2 and N1---H1B—N2 to form 1D chain along a axis as shown in Figure 4 whilst the hydrogen bond geometries are presented in Table 2.

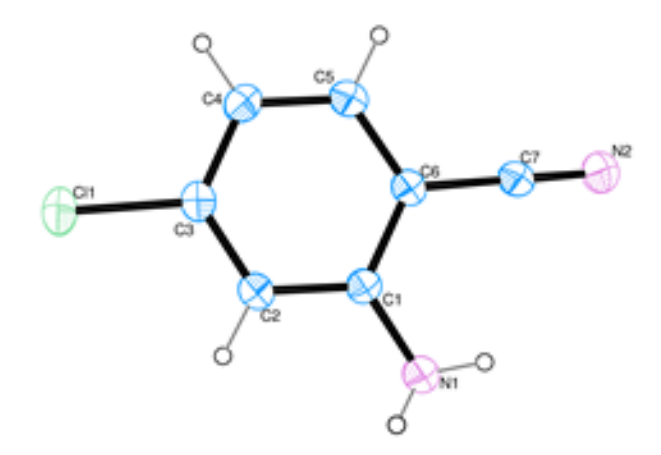


Figure 3. The molecular structure of ACBN with the atom labelling scheme. Displacement ellipsoids are drawn at the 50% probability level

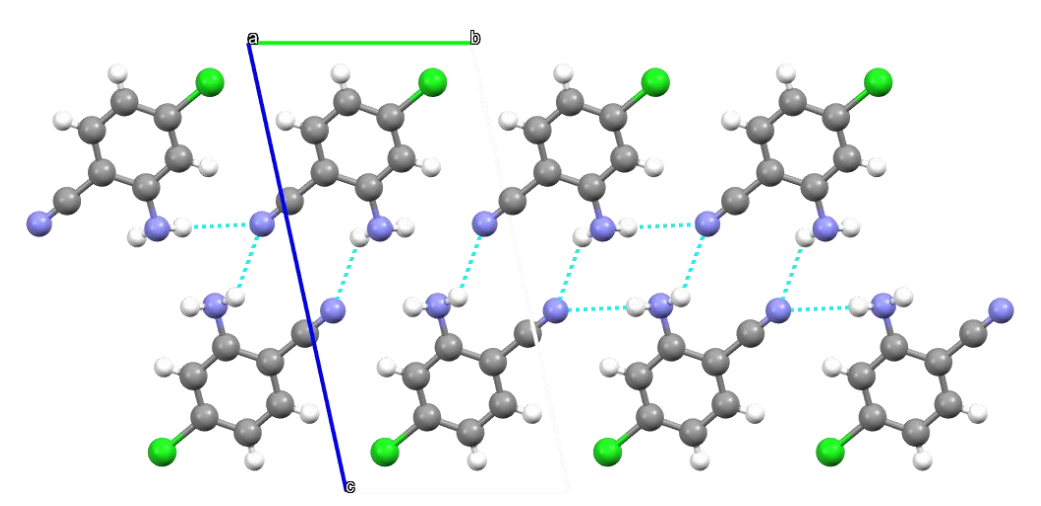


Figure 4. H-bonding view along a-axis

Table 1. Crystallographic data and structural refinement details of ACBN

Crystal Data			
Chemical Formula	C ₇ H ₅ ClN ₂		
Molecular mass (gmol ⁻¹)	152.58		
Crystal system, space group	Triclinic, P-1 293		
Temperature (K)			
a, b, c (Å)	3.8924 (9), 6.7886 (15), 13.838 (3)		
α, β, γ (°)	77.559 (16), 88.898 (17), 83.021 (17)		
$V(\mathring{A}^3)$	354.41 (14)		
Z	2		
Radiation type	$\begin{array}{c} M_o \ K_\alpha \\ 0.45 \\ 0.54 \ x \ 0.52 \ x \ 0.26 \end{array}$		
$\mu (mm^{-1})$			
Crystal size (mm)			
Tmin, Tmax	0.243, 0.267		
No. of measured, independent and observed [I> $2\sigma(I)$] reflections	6340, 2450, 1033		
R _{int}	0.080		
$(\sin \theta/\lambda) \max (\mathring{A}^{-1})$	0.750		
Refinement R[F ² > $2\sigma(F^2)$], wR(F ²), S	0.072, 0.158, 1.02		
$\Delta ho_{ m max}, \Delta ho_{ m min}$ (e Å ⁻³)	0.20, -0.24		

Table 2. Hydrogen bond geometries of ACBN

D–H···A	D–H (Å)	H…A (Å)	D…A (Å)	D-H···A (°)	Symmetry Codes
N1-H1A···N2	0.86	2.5	3.166(4)	135	2-x,-y,1-z
N1-H1B···N2	0.86	2.53	3.375(4)	168	x,1+y,z

Hirshfeld surface analysis

The Hirshfeld Surface Analysis was performed to quantify the nature of the intermolecular interactions [16]. Figure 5 presents the Hirshfeld Surface mapped over dnorm. The deep red spots on the dnorm Hirshfeld surfaces represent the close contact interactions, which are mainly responsible for the significant intermolecular N-H···N interactions. The Hirshfeld surfaces mapped over the shape index (Figure 6a) shows comparatively weak interactions involving the phenyl rings represented by the yellowish triangular-shaped regions, which indicate that $\pi \cdots \pi$ stacking interactions are present in the crystal packing. The $\pi \cdots \pi$ stacking interaction is significant as the Cg1-to-Cg1 separation ranges from 3.892(2) to 3.893(2) Å [17]. The Cg1 represents the centroid of C1, C2, C3, C4, C5 and C6. The presence of this $\pi \cdots \pi$ stacking interactions is also evident by the map of curvedness (Figure 6b) which shows flat surface patches. Two-dimensional fingerprint plots from the Hirshfeld surface analysis of this title compound were calculated to gain quantitative data on the percentage contributions of different intermolecular interactions to the overall Hirshfeld surfaces. The overall twodimensional fingerprint plot that represents intermolecular contacts are illustrated in Figure 7. The most dominant contribution (26.7%) originates from N···H/H···N contacts which signify the presence of N-H...N interactions. The Cl...H/H...Cl contacts are observed at 21.3% while H···H contacts at 17.9%. The other contacts which are H···C/C···H, C···C, Cl···Cl, $N\cdots C/C\cdots N$, $Cl\cdots C/C\cdots Cl$ and $N\cdots N$, show the percentage contributions of 12.3%, 10.8%, 4.2%, 2.6%, 2.3% and 2%, respectively. All these interactions contribute a significant role in crystal packing.

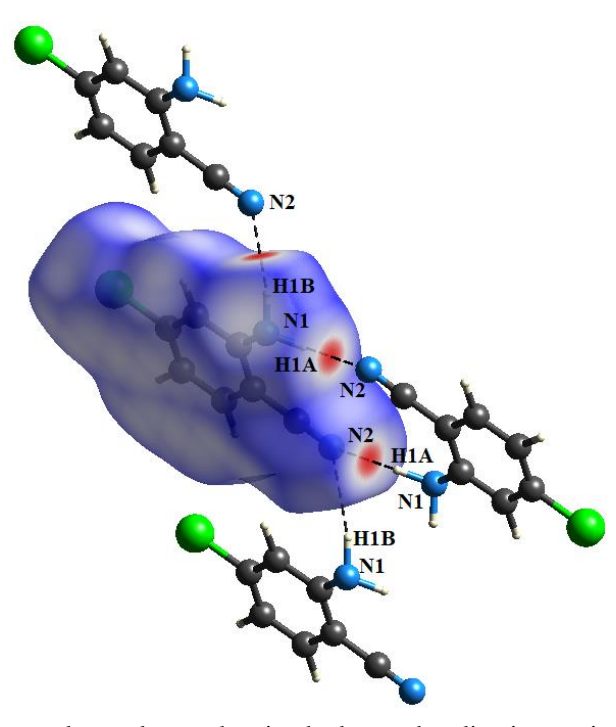


Figure 5. Hirshfeld surfaces mapped over dnorm showing hydrogen-bonding interactions (black dash line) with their neighbouring molecules

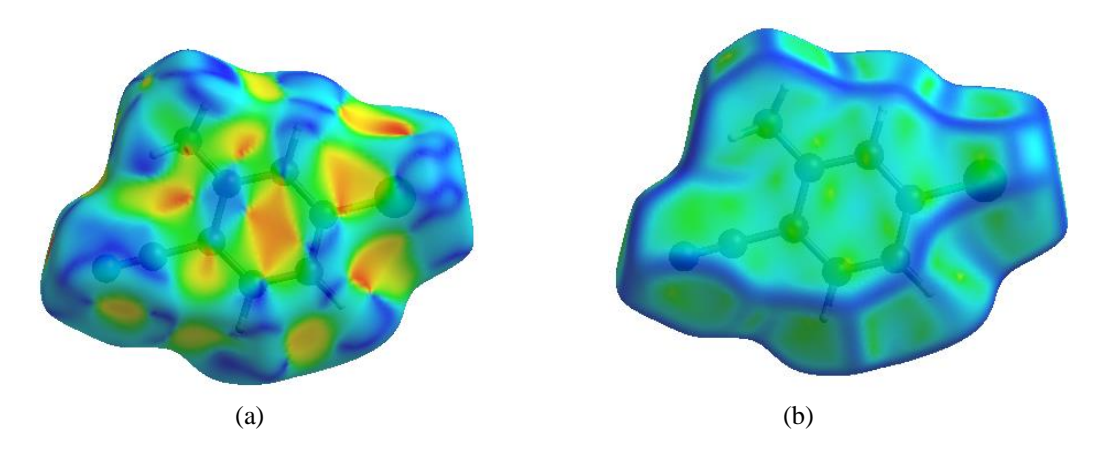


Figure 6. Hirshfeld surfaces mapped over (a) shape index and (b) curvedness

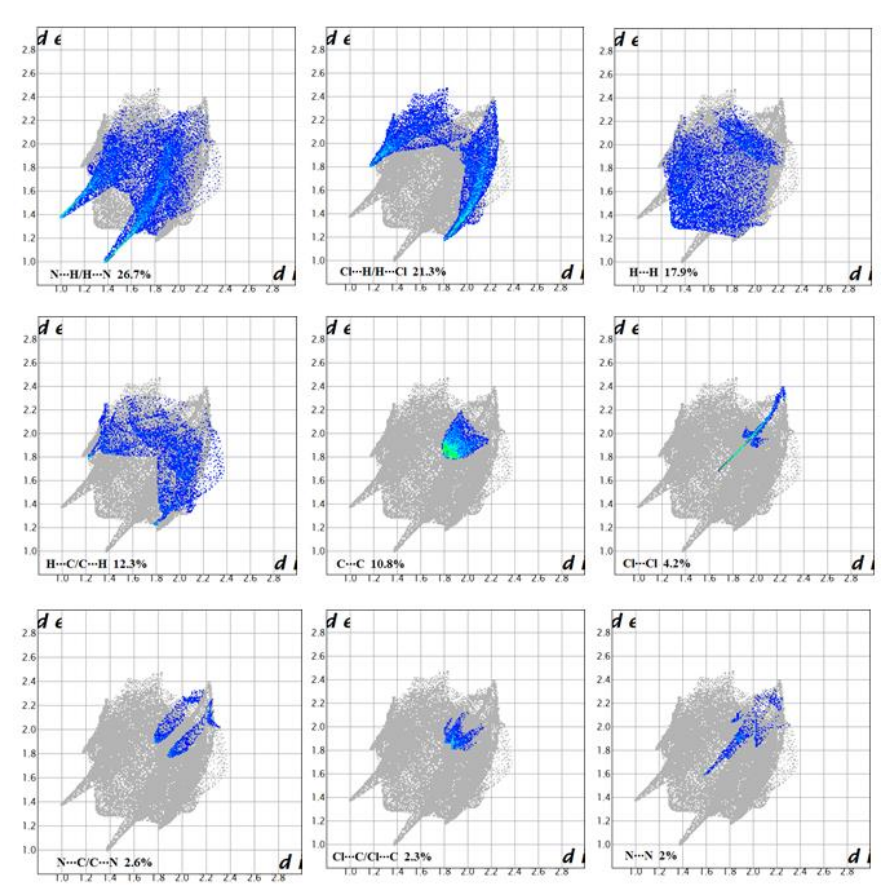


Figure 7. Two-dimensional fingerprint plots of the title compound with their respective contributions

Density functional theory: Mulliken population method

The Mulliken population method using B3LYP/6-311++G(d,p) level of calculation was successfully calculated to obtain the total atomic charge distribution of ACBN. As shown in Figure 8, the 7 atoms from ACBN exhibit negative charges namely 1C, 3C, 4C, 6C, 11N, 14C, and 15N. Positive charges are found in 2C, 5C, 7H, 8H, 9H, 10Cl, 12H, and 13H. The result showed that atom 15N and 11N have a high tendency to act as a nucleophilic atom for the compound as they have negative charges with values of -0.202 and -0.237, respectively.

Intrinsic molecular characteristics

The global reactivity parameters of ACBN are shown in Table 3. The HOMO and LUMO electrons were primarily localized across the whole ACBN. The greater values of ionization potential, I and electron donating

capability (ω) showed that the ACBN has the capability to donate rather than accept the electrons [18]. Hence, it has the capability to form complexes easier. In comparison to literature, the energy gap value, ΔE , resolved from the crystal data is lower at 3.4988 eV. Sudha et al. [19] generated DFT data using the proposed structure, while this study used crystal data. Calculated ΔE is a crucial stability indicator that aids in defining the compound's chemical reactivity and kinetic stability [20]. As the ΔE value of ACBN is lower than that of the previous study, the reactivity rises with a greater degree of electronic charge transfer from the ACBN as a free ligand to the central metal ion, making it easier to provide electrons to an acceptor. Sherif and Abdel-Kader et al. [21] stated that the ACBN undergoes conjugation, which contributes to the low value of the

energy gap as well. The ACBN has very strong electrophilic properties since the global electrophilicity value is more than 1.5 eV [22]. Global hardness (η) and softness (S) are frequently employed to assess the stability and reactivity of compounds. The ACBN is categorized as a hard compound because the value of global hardness (η) is larger than global softness (S).

The high hardness value consistently suggests greater stability and lessened reactivity. It is also consistent with the high value of chemical potential. But despite the high value of ω , the ACBN still shows potential to donate electrons to other compounds for specific applications.

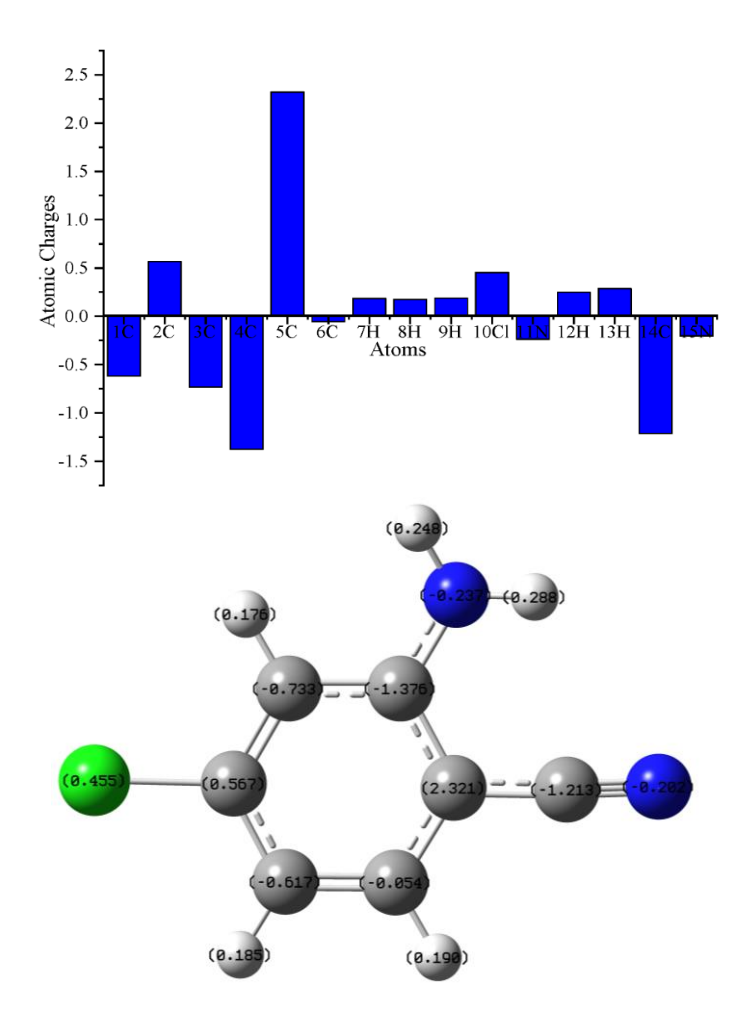


Figure 8. Optimized structure and bar diagram representing the charge distribution of ACBN

Table 3. Global reactivity parameters of ACBN

Molecular energy (eV)	ACBN Molecular energy (eV)		ACBN
Еномо	-8.1171 eV	Global Softness (S)	0.1570 eV ⁻¹
E_{LUMO}	-4.6183 eV	Chemical potential (µ)	-6.3677 eV
Energy gap (ΔE)	3.4988 eV	Electronegativity (χ)	6.3677 eV
Ionization potential (I)	8.1171 eV	Global electrophilicity (ω)	11.589 eV
Electron affinity (A)	4.6183 eV	Electron donating capability (ω ⁻)	14.992
Global hardness (η)	1.7494 eV	Electron accepting capability (ω^+)	8.6238

Molecular electrostatic potential

The nitrile (C\(\exists N\)) is identifiable as a high electron density region as shown in Figure 9, indicating the most preferable reactivity for nucleophilic site. Besides that,

the proton of NH₂ has a very noticeable low electron density, which indicates the most preferable reactivity for an electrophilic site [23].

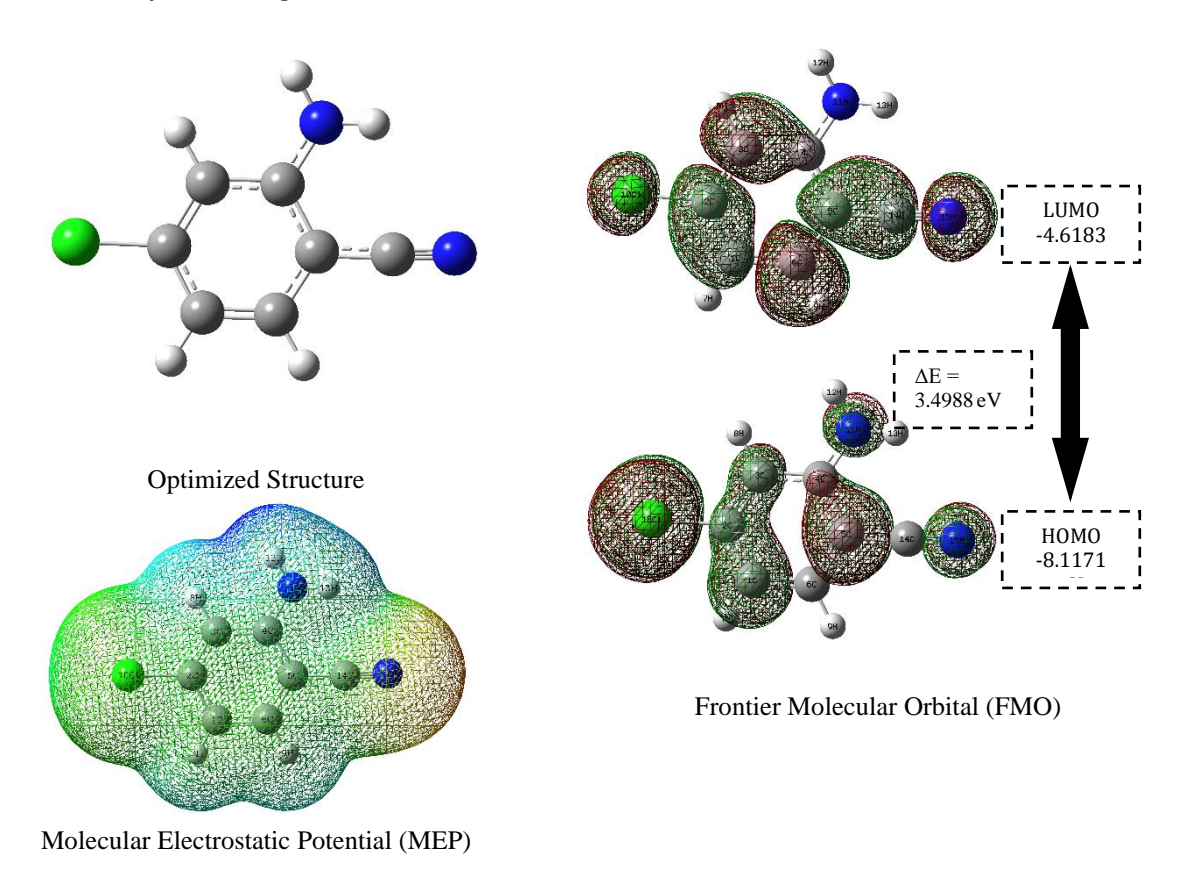


Figure 9. The optimized structure, MEP and FMO of ACBN

Conclusion

The crystal structure of 2-amino-4chlorobenzonitrile (ACBN) was successfully confirmed spectroscopic and single crystal X-ray crystallographic studies. The Hirshfeld Surface analysis revealed that $N \cdots H/H \cdots N$ contacts are the most dominant contributions to the total Hirshfeld surfaces which signify the presence of $N-H\cdots N$ interactions. The intrinsic molecular characteristics analysis showed that although the ACBN is stable and less reactive, the compound still shows a potential in transferring and accepting electrons. Besides that, the Mulliken study showed that the compound has the potential to act as a nucleophilic agent through the nitrogen atoms (highly negative charges). As recommendation, the DFT study

revealed that the compound could be investigated more thoroughly in terms of reaction kinetics and mechanisms such as corrosion inhibition and biological activities.

Acknowledgement

The authors thank Ondokuz Mayıs University (Turkey) for the single-crystal X-ray experiment and the Experimental and Theoretical Research Laboratory, International Islamic University Malaysia, for providing the computational facility.

Supplementary Data

CCDC-2224917 contains the supplementary crystallographic data for the compound reported in this paper. These data can be obtained free of charge at

www.ccdc.cam.ac.uk/conts/ retrieving.html [or from the Cambridge Crystallographic Data Centre (CCDC), 12 Union Road, Cambridge CB2 1EZ, UK; fax:+44(0)1223-336033; e-mail: deposit@ccdc.cam.ac.uk].

References

- Sundaraganesan, N., Elango, G., Sebastian, S. and Subramani, P. (2009). Molecular structure, vibrational spectroscopic studies and analysis of 2fluoro-5-methylbenzonitrile. *Indian Journal of Pure & Applied Physics*, 47: 481-490.
- Misra, N., Ahmad Siddiqui, S., Pandey, A. K. and Trivedi, S. (2009). Comparative vibrational spectroscopic investigation of benzonitrile derivatives using density functional theory. *Der Pharma Chemica*, 1(1): 196-209.
- Kumar, V., Panikar, Y., Palafox, M. A., Vats, J. K., Kostova, I., Lang, K. and Rastogi, V. K. (2010). Ab-initio Calculations, FT-IR and FT-raman spectra of 2-chloro-6-methyl benzonitrile. *Indian Journal of Pure and Applied Physics*, 48: 85-94.
- 4. Dixon, A. R., Khuseynov, D. and Sanov, A. (2015). Benzonitrile: Electron affinity, excited states, and anion solvation. *Journal of Chemical Physics*, 143(13): 1-12.
- Karaağaç, D. (2021). Preparation and characterisation of the cyano-bridged transition metal complexes using *n,n'*-diethyl thiourea as a ligand. *South African Journal of Chemistry*, 75: 130-135.
- Hirose, M. And Torii, H. (2022). Role of the electrostatic interactions in the changes in the CN stretching frequency of benzonitrile interacting with hydrogen-bond donating molecules. *Journal of Molecular Liquids*, 362: 1-7.
- Stoe and Cie (2002) X-AREA (Version 1.18) X-RED32 (Version 1.04) Stoe & Cie, Darmstadt, Germany.
- 8. Sheldrick, G. M. (2008) A short history of SHELX, *Acta Crystallographica*, A64: 112-122.
- 9. Farrugia, L. J. (1997). ORTEP-3 for Windows a version of ORTEP-III with a Graphical User Interface (GUI). *Journal of Applied Crystallography*, 30(5): 565.

- Macrae, C. F., Edgington, P. R., McCabe, P., Pidcock, E., Shields, G. P., Taylor, R., Towler, M., van de Streek, J. and Streek, J. V. D. (2006) Mercury: Visualization and analysis of crystal structures. *Journal of Applied Crystallogarphy*, 39: 453-457.
- Turner, M. J., McKinnon, J. J., Wol, S. K., Grimwood, D. J., Spackman, P. R., Jayatilaka, D. and Spackman, M. A. (2017). Crystal Explorer 17, University of Western Australia: Crawley, Australia.
- 12. Vhanale, B., Kadam, D. and Shinde, A. (2022) Synthesis, spectral studies, antioxidant and antibacterial evaluation of aromatic nitro and halogenated tetradentate Schiff bases. *Heliyon*, 8(6): 1-7.
- 13. Geethapriya, J., Devaraj, A. R., Gayathri, K., Swadhi, R., Elangovan, N., Manivel, S., Sowrirajan, S. and Thomas, R. (2023). Solid state synthesis of a fluorescent Schiff base (*E*)-1-(perfluorophenyl)-*N*-(*o*-toly)methanimine followed by computational, quantum mechanical and molecular docking studies. *Results in Chemistry*, 5: 1-11.
- 14. Nayak, S. G. and Poojary, B. (2019). Synthesis of novel Schiff bases containing arylpyrimidines as promising antibacterial agents. *Heliyon*, 5: 1-7.
- Đorović, J., Marković, Z., Petrović, Z. D., Simijonović, D. and Petrović, V. P. (2017). Theoretical analysis of the experimental UV-Vis absorption spectra of some phenolic Schiff bases. *Molecular Physics*, 115(19): 2460-2468.
- 16. Nasaruddin, N. H., Ahmad, S. N., Sirat, S. S., Wai Tan, K., Zakaria, N. A., Mohamad Nazam, S. S., Abd Rahman, N. M. M., Mohd Yusof, N. S. and Bahron, H. (2022). Synthesis, structural characterization, Hirshfeld surface analysis, and antibacterial study of Pd(II) and Ni(II) Schiff base complexes derived from aliphatic diamine. ACS Omega, 7(47): 42809-42818.
- Hema, M. K., García-Santos, I., Castiñeiras, A., Mehrabian, M., Zangrando, E., Ramalingam, R. J., Ramakrishna, B. N., Lokanath, N. K., Karthik, C. S., Mahmoudi, G. (2023) Cg...Cg interactions driven 1D polymeric chains bridged by lattice solvents in N³-(2-pyridoyl)-4-

Dogan et al.: SPECTROSCOPIC, CRYSTAL STRUCTURE, HIRSHFELD SURFACE AND DFT STUDIES OF 2-AMINO-4-CHLOROBENZONITRILE

- pyridinecarboxamidrazone Pb(II) complex. *Journal of Molecular Structure*, 1294(1): 136420-136429.
- Razali, N. Z. K., Sheikh Mohd Ghazali, S. A. I., Sharif, I., Sapari, S., Abdul Razak, F. I. and Dzulkifli, N. N. (2022). Synthesis, characterisation and corrosion inhibition screening on 2chloroacetophenone 4-ethyl-3-thiosemicarbazone: Morphology, weight loss and DFT studies. Chemical Papers, 76: 5955-5966.
- 19. Sudha, S., Sundaraganesan, N., Kurt, M., Cinar, M. and Karabacak, M. (2011). FT-IR and FT-Raman spectra, vibrational assignments, NBO analysis and DFT calculations of 2-amino-4-chlorobenzonitrile. *Journal of Molecular Structure*, 985:148-156.
- 20. Rakha, T. H., El-Gammal, O. A., Metwally, H. M. and Abu El-Reash, G, M. (2014). Synthesis, characterization, DFT and biological studies of (*Z*)-*N*·-(2-oxoindolin-3-ylidene)picolinohydrazide and

- its Co(II), Ni(II) and Cu(II) complexes. *Journal of Molecular Structure*, 1062: 96-109.
- Sherif, O. E. and Abdel-Kader, N. S. (2018). DFT calculations, spectroscopic studies, thermal analysis and biological activity of supramolecular Schiff base complexes. *Arabian Journal of Chemistry*, 11(5):700-713.
- 22. Domingo, L. R., Aurell, M. J., Perez, P. and Contreras, R. (2002). Quantitative characterization of the global electrophilicity power of common diene/dienophile pairs in diels-alder reactions. *Tetrahedron*, 58: 4417-4423.
- 23. Idelfitri, N. I. F., Dzulkifli, N. N., Ash'ari, N. A. N., Sapari, S., Abdul Razak, F. I. and Pungot, N. H. (2023). Synthesis, characterisation and corrosion inhibitory study of meldrum's acid thiosemicarbazone: Weight loss, SEM-EDX and DFT. *Inorganic Chemistry Communications*, 150: 1-11.